The Journal of Antibiotics (2016) 69, 637–646

www.nature.com/ja

ORIGINAL ARTICLE

Quinovosamycins: new tunicamycin-type antibiotics in which the α, β-1″,11′-linked *N*-acetylglucosamine residue is replaced by *N*-acetylquinovosamine

Neil PJ Price[1], David P Labeda[2], Todd A Naumann[2], Karl E Vermillion[3], Michael J Bowman[4], Mark A Berhow[3], William W Metcalf[5,6] and Kenneth M Bischoff[1]

Tunicamycins (TUN) are potent inhibitors of polyprenyl phosphate *N*-acetylhexosamine 1-phosphate transferases (PPHP), including essential eukaryotic GPT enzymes and bacterial HexNAc 1-P translocases. Hence, TUN blocks the formation of eukaryotic *N*-glycoproteins and the assembly of bacterial call wall polysaccharides. The genetic requirement for TUN production is well-established. Using two genes unique to the TUN pathway (*tunB* and *tunD*) as probes we identified four new prospective TUN-producing strains. Chemical analysis showed that one strain, *Streptomyces niger* NRRL B-3857, produces TUN plus new compounds, named quinovosamycins (QVMs). QVMs are structurally akin to TUN, but uniquely in the 1″,11′-HexNAc sugar head group, which is invariably D-GlcNAc for the known TUN, but is D-QuiNAc for the QVM. Surprisingly, this modification has only a minor effect on either the inhibitory or antimicrobial properties of QVM and TUN. These findings have unexpected consequences for TUN/QVM biosynthesis, and for the specificity of the PPHP enzyme family.
The Journal of Antibiotics (2016) **69,** 637–646; doi:10.1038/ja.2016.49; published online 18 May 2016

INTRODUCTION

There is a definite need for new drugs to treat infections due to bacteria that are resistant to existing antibiotics. In addition, the development of new antibiotics, particularly those with a novel mode of action, has slowed considerably. This is exacerbated by the rapid emergence of bacterial resistance to new drugs as they are introduced, and for the five most recent antibiotics this has occurred within 1 year of their introduction.[1] One approach to future drug leads is data mining of large genomic data sets, especially those from *Actinomycetes*, which contain a wealth of natural product biosynthetic gene clusters.[2,3] Hence, genomic-enhanced discovery has led to the identification of phosphonate-based anti-metabolites and to the occurrence of uncommon biosynthetic pathways for nonribosomal peptides and polyketides.[4–6]

Tunicamycins (TUNs) are a heterologous family of nucleoside antibiotics that target the early stages of biosynthesis for bacterial peptidoglycan and eukaryotic *N*-glycoproteins.[7–9] The mode of action is known, with the TUN–Mg^{2+} complex established as a transition state analog for several hexosamine-1-phosphate:prenol phosphate translocases.[10,11] A biosynthetic pathway has been proposed for TUN in which the 11-carbon dialdose sugar, tunicamine, is derived from uridine and *N*-acetylglucosamine.[12–14] The pseudoribosyl ring of tunicamine is *N*-glycosidically linked to uracil to form a structure highly analogous to the nucleoside uridine, and is presumed to mimic the UMP leaving group in the transition state for the translocase-catalyzed reactions. This inhibits the formation of *N*-acetylmuramyl-pentapeptide-undecaprenyl pyrophosphate in bacteria or *N*-acetylglucosamine-dolichol pyrophosphate in eukaryotes, which are essential intermediates in these organisms.[15–17]

Here, we present a data mining analysis of a large genomic library of *Actinomyces* genomes to identify several new TUN-producing actinomycetes strains. Chemical and spectrometric analysis of the fermentation products from one of these strains, *Streptomyces niger* NRRL B-3857, revealed that it uniquely produces a novel family of TUN-like compounds that we have named quinovosamycins (QVMs). We report the purification and structural characterization of three QVMs, and we present structural and antimicrobial comparisons with three TUNs that are also isolated from *S. niger*. The relevance of the structure of these new compounds to TUN biosynthesis is discussed, as is their unexpectedly potent activity against *Bacillus subtilis* and *Saccharomyces cerevisiae*. These findings challenge the current paradigm for the high selectivity of the Asn-linked GlcNAc residue in eukaryotic *N*-glycoprotein assembly, and also provide a basis for studying the specificity and selective inhibition of bacterial

[1]Renewable Products Technology Unit, National Center for Agricultural Utilization Research, USDA-ARS, Peoria, IL, USA; [2]Mycotoxin Prevention and Applied Microbiology Unit, National Center for Agricultural Utilization Research, USDA-ARS, Peoria, IL, USA; [3]Functional Foods Unit, National Center for Agricultural Utilization Research, USDA-ARS, Peoria, IL, USA; [4]Bioenergy Research Unit, National Center for Agricultural Utilization Research, USDA-ARS, Peoria, IL, USA; [5]Department of Microbiology, University of Illinois at Urbana-Champaign, Urbana, IL, USA and [6]Institute for Genomic Biology, University of Illinois at Urbana-Champaign, Urbana, IL, USA
Correspondence: Dr NPJ Price, Renewable Products Technology Unit, National Center for Agricultural Utilization Research, USDA-ARS, 1815N. University Street, Peoria, IL 61604, USA.
E-mail: neil.price@ars.usda.gov
Received 25 January 2016; revised 22 March 2016; accepted 3 April 2016; published online 18 May 2016

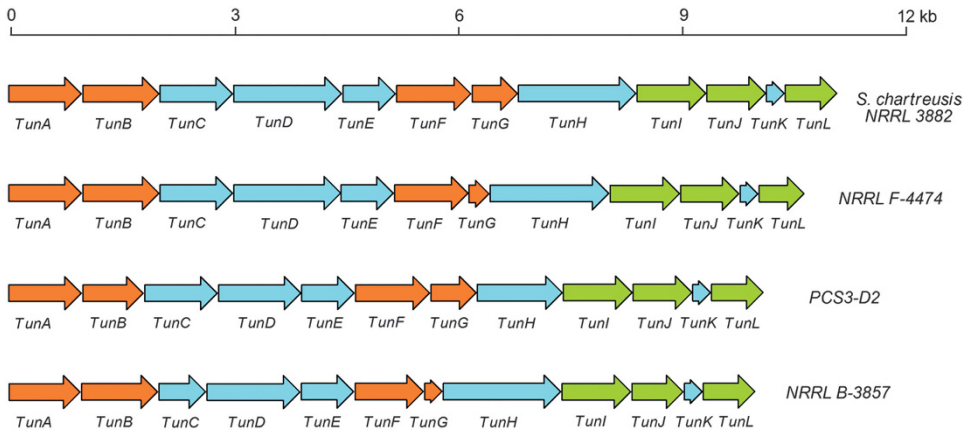

Figure 1 Genetic organization of the tunicamycin biosynthetic operons of strains *S. chartreusis* NRRL B-3882, *Streptomyces* sp. NRRL F-4474, *Streptomyces* sp. PCS3-D2 and *S. niger* NRRL B-3857.

polyprenyl phosphate *N*-acetylhexosamine 1-phosphate transferase family members.

RESULTS

Bioinformatic analysis using *tunB* and *tunD* gene sequences to probe an actinomycetes genomic library

The TUN biosynthetic operon of 12 essential *tun* genes (*tunA–tunL*) has been characterized in several diverse actinomycetes,[13,14,18] and TUN production is known to occur in various other actinobacteria.[8,19] Two genes, encoding for a radical SAM protein (TunB) and an unusual α–β-anomeric-to-anomeric glycosyltransferase (TunD) are highly selective to the TUN pathway.[13,14] The catalytic activity of TunB is to generate the 11-carbon sugar tunicamine from 6-carbon 5′,6′-exo-glycal intermediates which are themselves generated from UDP-GlcNAc.[20] Using the *tunB* and *tunD* gene sequences as probes of an actinomycetes genomic library we identified seven microorganisms with the potential for TUN biosynthesis, four of which are previously unreported. These include *Streptomyces* sp. NRRL F-4474, *Streptomyces niger* NRRL B-3857 (formally *Chainia nigra*), *Streptomyces* sp. PCS3-D2 and *Nocardia nova* SH22a, a bacterium capable of degrading gutta-percha and natural rubber.[21] The size and organization of *tunA* through *tunL* genes is analogous in three of these strains (Figure 1), although the *tunD* and *tunH* genes suffer from poor assemblies of the draft genome data in PCS3-D2, with strings of NNNs interrupting the coding sequence. The evidence suggests that there are no qualitative differences in the biosynthetic operon in these strains compared with those in TUN-producing strains identified earlier.[18] By contrast, although *tunB* and *tunD* homologs are present on the *Nocardia nova* genome several of the other tun genes (*tunC, E, K, L*) are absent. An incomplete tun operon lacking a *tunL* gene has been described previously for *Actinosynnema mirum*,[13,14] and we note that this strain is unable to produce TUNs (data not shown).

Structural analysis using MS (MALDI/MS, LC/MS, MS/MS, permethylation analysis) and HPLC purification of QVMs

On the basis of the genetic analysis, we decided to investigate two of the strains in more detail. Matrix-assisted laser desorption/ionization MS (MALDI/MS) analysis of an acid-precipitated methanolic fraction from fermentation of *Streptomyces* sp. F-4474 identified the known TUNs Tun-14:1–Tun-17:1 (data not shown), as previously found from *S. chartreusis* and *S. lysosuperificus* strains.[22] Similarly, MALDI/MS analysis of *S. niger* NRRL B-3857 extracts identified TUNs Tun-15:1 ($(M+Na)^+ = m/z$ 853.6, T1), Tun-16:1 ($(M+Na)^+ = m/z$ 867.7, T2), and Tun-17:1 ($(M+Na)^+ = m/z$ 881.6, T3; Figure 2a). These T-series ions differ by 14 Da, characteristic of the —CH_2— chain length difference in the *N*-acyl group. However, a second series (Q-series) of molecular ions is also apparent at *m/z* 837.6 (Q1), *m/z* 851.6 (Q2) and *m/z* 865.6 (Q3) that also differ in mass by a —CH_2— unit and, in addition, are 16 Da smaller than the corresponding TUN components (Figure 2a). Reversed-phase HPLC separation indicated that the Q-series components are more lipophilic than the corresponding T-series, typically eluting from the column about 0.5 min later (Figure 2b). Hence the T-series TUNs were eluted as fractions 1, 3 and 5, whereas the corresponding Q-series components were in the slower eluting fractions 2, 4 and 6, as is clear from the MALDI/MS analyses of these fractions (Figure 2c). Moreover, we observed by MALDI/MS that after peracetylation of the fermentation products, 7 acetyl groups were incorporated into the Q-series compounds ($(M+(42\times7)+Na)^+$ ions $= m/z$ 1131.6, 1145.6 and 1159.6), whereas 8 acetyls were added for the T-series ($(M+(42\times8)+Na)^+$ ions $= m/z$ 1189.6, 1203.6 and 1217.6; Supplementary information, Figure S2). Taken together, these data indicate that the Q-series compounds have one less hydroxyl group than the corresponding TUN.

The composition of the HPLC-purified fractions were further analyzed by LC/MS^n under a variety of ion-fragmentation conditions (Figure 3). MS^1 analysis of pseudomolecular $(M+H)^+$ ions identified T-series ions at *m/z* 831.3 (T1), *m/z* 845.3 (T2) and *m/z* 857.3 (T3), with corresponding MS^2 ions 221 Da smaller at *m/z* 610.3 (T1–221), *m/z* 624.3 (T2–221) and *m/z* 638.3 (T3–221). This 221 Da mass difference is due to a neutral loss of the α, β-1″,11′-linked *N*-acetylglucosamine residue from the parent TUN ions (Figure 3).[22] LC/MS^1 analysis of the Q-series components identified *m/z* 815.2 (Q1), *m/z* 829.2 (Q2) and *m/z* 843.3 (Q3) as the molecular ions, but in this case with a corresponding MS^2 loss of 205 Da, as seen at *m/z* 610.3 (Q1–205), *m/z* 624.3 (Q2–205) and *m/z* 638.3 (Q3–205; Figure 3). Further fragmentation of the MS^2 ions produced MS^3 ions and subsequently MS^4 ions that are the same for both T-series TUNs and the Q-series compounds. These data indicated that, other than the *N*-acyl chains, the structures of T- and Q-series components differ only in the identity of the 1″,11′-linked glycosidic residue, which generates a neutral mass of 221 Da due to GlcNAc for the TUNs, and of 205 Da (deoxyHexNAc) for the corresponding masses of the Q-series compounds.

Additional evidence supporting the presence of a deoxyHexNAc in the Q-series compounds came from analysis of permethylated components. LC-MS of the permethylated analytes of the T-series

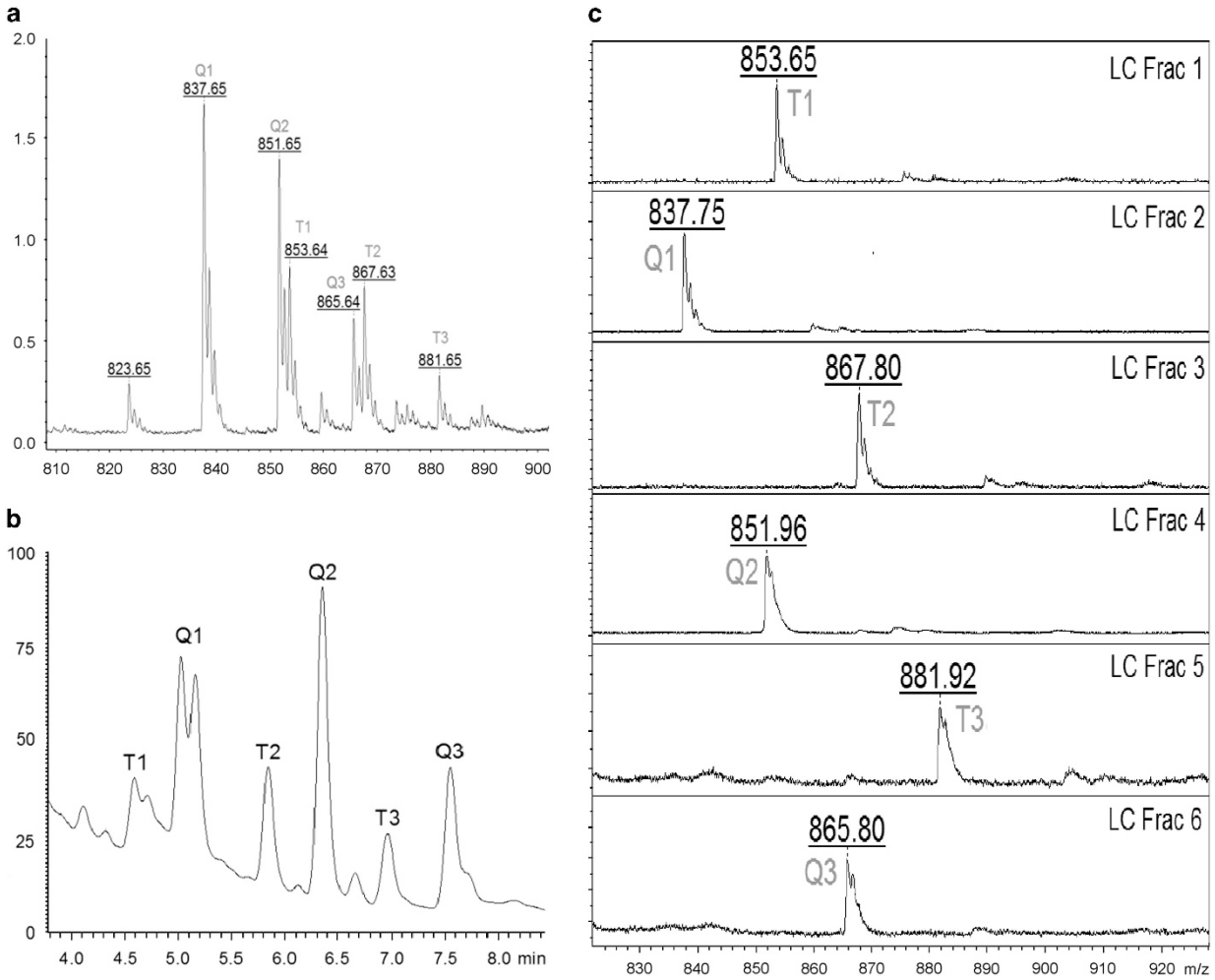

Figure 2 Identification and purification of the quinovosamycins (Q1, Q2 and Q3) and tunicamycins (T1, T2 and T3) from the fermentation broth of *Streptomyces niger* NRRL B-3857. (**a**) MALDI-TOF/MS of the acidified methanolic extract of the *S. niger* cell pellet. Sodium adduct ions *m/z* 837.65, 851.65 and 865.64 are due to QVM-15:1, QVM-16:1 and QVM-17:1, and *m/z* 853.64, 867.63 and 881.65 are due to TUN-15:1, TUN-16:1 and TUN-17:1, respectively. (**b**) Purification of isolated QVM and TUN components by C18 reversed-phase HPLC. (**c**) MALDI-TOF/MS analysis of the individual components after HPLC purification. A full color version of this figure is available at *The Journal of Antibiotics* journal online.

($(M+Na)^+$ *m/z* 993.6 (T1); 1007.6 (T2); 1021.6 (T3)) and the Q-series ($(M+Na)^+$ *m/z* 963.6 (Q1); 977.6 (Q2); 991.6 (Q3)) revealed that the Q-series was 30 Da lower in mass, consistent with the lack of a hydroxyl group (−16 Da) and the loss of the methylation site (−14 Da) for the hydroxyl group (Supplementary information, Figure S3). The dominant fragment ion of the LC-MS^2 spectra of the permethylated T- and Q-series was the loss of 277 Da (permethylated HexNAc) and 247 Da (permethylated deoxyHexNAc), respectively; thereby further establishing the position of the modification. All subsequent fragmentations (MS^3–MS^5) were identical in fragment ions and intensities for both T- and Q-series spectra. These data provide strong evidence for the presence of a deoxyHexNAc on the Q-series analytes at the 1″,11′-linked glycosidic residue.

Chemical synthesis of 6-Deoxy-D-HexNAc standards for comparative carbohydrate analysis by GC/EI-MS.

The observed 16-Da difference in the masses of the neutral MS^2 losses suggested that the Q-series compounds from *S. niger* might contain a deoxy *N*-acetylhexosamine residue in place of the TUN 1″,11′-GlcNAc group, but did not provide insight into the possible stereochemistry for this sugar. To the best of our knowledge *N*-acetylfucosamine (FucNAc) and *N*-acetylquinovosamine (QuiNAc) are the most common 6-deoxy *N*-acetylhexosamines that occur biologically, but these were unavailable as chemically defined standards. We therefore synthesized D-QuiNAc and D-FucNAc from D-GlcNAc and D-GalNAc, respectively, using a modification of the Ponpipom–Hanessian procedure. Essentially, the parent *N*-acetylhexosamines were 6-brominated with *N*-bromosuccinimide in the presence of triphenylphosphine in anhydrous dimethylformamide, and subsequently catalytically hydrogenated in the presence of Pd/C.[23,24] The products were peracetylated *in situ* and subsequently analyzed by GC/MS. In addition, the starting material sugars, the 6-bromo intermediates, and the products were converted to aldononitrile acetates (PAANs) and analyzed by GC/MS in electron impact (EI) ionization mode. The 6-deoxysugar standards produced in this way were compared by GC/MS with the natural aminosugar component obtained by acid hydrolysis of the HPLC-purified QVM and TUN components from *S. niger* (Figure 4). Noticeably, the aminosugar from the Q-series compounds co-eluted with the D-QuiNAc standard with a retention time (R_t) of 10.85 min, and is well-separated from the D-FucNAc standard at R_t 12.0 min

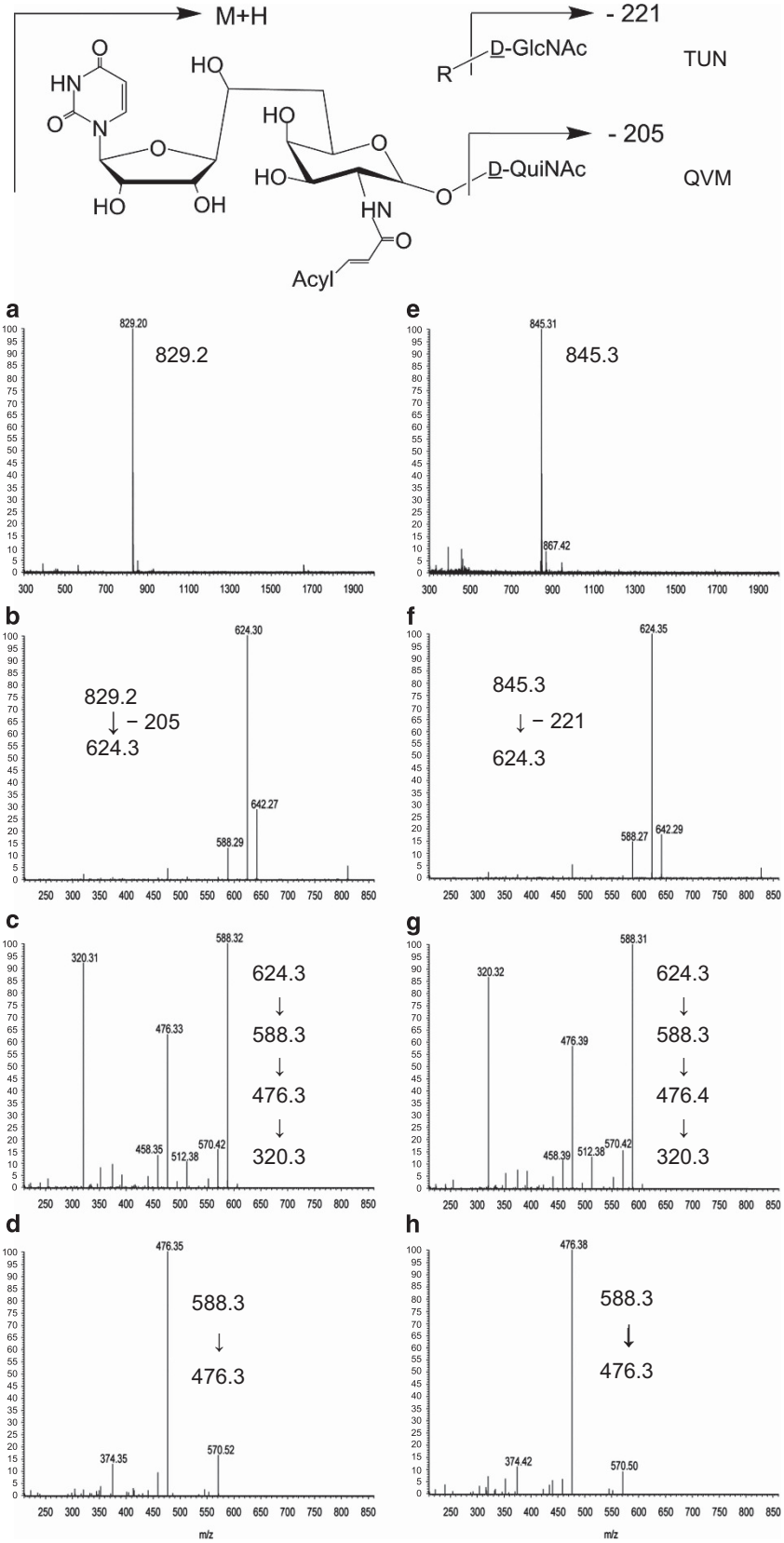

Figure 3 LC/MS^n analysis of quinovosamycin Q2 (QVM-16:1, $(M+H)^+ = m/z$ 829.2 (**a**–**d**)), and tunicamycin T2 (TUN-16:1, $(M+H)^+ = m/z$ 845.3 (**e**–**h**)). MS^2 neutral losses of 205 Da (m/z 829.2 → 624.3 (**b**)) or 221 Da (m/z 845.3 → 624.3; (**b**)) arise from the α1″,11′-QuiNAc or -GlcNAc, respectively (schematic inserted at top). Subsequent MS^3 (**c**, **g**) and MS^4 (**d**, **h**) fragmentation pathways are identical, consistent with the core structural similarities of QVM and TUN.

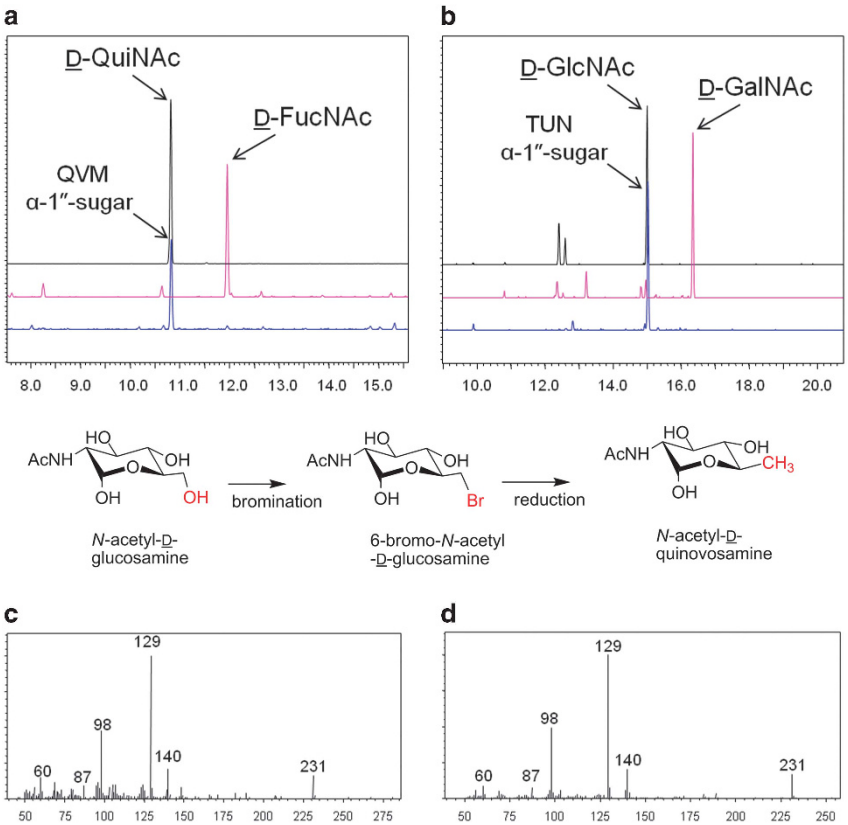

Figure 4 GC/MS analysis of the QVM/TUN α1″,11′-linked HexNAc. Acid-hydrolyzed QVM (**a**) or TUN (**b**) were analyzed as their aldononitrile acetate derivatives. D-QuiNAc and D-FucNAc standards were prepared from GlcNAc and GalNAc, respectively, by bromination/reduction under Ponpipom conditions.[23] EI-MS spectra of the aldononitrile acetates of synthetic QuiNAc (**c**) and the QuiNAc from acid-hydrolyzed QVM (**d**).

(Figure 4). The parent D-GlcNAc and D-GalNAc sugars eluted later under these conditions (R_t 15.00 min and R_t 16.20 min, respectively), with the native sugar from the acid-hydrolyzed T-series TUNs co-eluting as expected with the D-GlcNAc. Hence, the 6-deoxy *N*-acetylhexosamine sugar residue found on the Q-series compounds from *S. niger* is *N*-acetylquinovosamine, and consequently these compounds are named QVMs. The GC/MS analysis also identified uracil as a component in the acid-hydrolyzed TUNs and QVMs, confirming that uracil rather than 5,6-dideoxyuracil (5,6-DHU) is the nucleoside motif for both of these molecules. 5,6-DHU has previously been identified as an alternative base of other diverse TUNs, the streptovirudins,[25] although differences in the 1″,11′-*N*-acetylhexosamine residue has not been described previous.

Structural analysis of QVMs using NMR

A suite of NMR data (^{1}H, ^{13}C, COSY, HSQC, HMBC and TOCSY) was obtained on the HPLC-purified TUNs and QVMs from *S. niger*, and compared with corresponding spectra of commercial TUN which was obtained from *S. chartreusis* NRRL B-3882 (Figure 5, Supplementary Table S1). We have previously reported the conformation of TUN using a combination of NMR analysis and metabolic labeling from chirally deuterated substrates.[11] The NMR spectra for TUN are characterized by four spin system: the 11-carbon tunicamine sugar, the uracil ring, the α1′′,β11′-*N*-acetylglucosamine; and the *N*-acyl group. The characteristic anomeric-to-anomeric α1′′, β11′-glycosidic bonds are highly unusual, and for TUN these are evident from the GlcNAc α1′′-anomeric proton at 5.04 p.p.m. (C-1′′, 100.3 p.p.m.) and the tunicamine β11′-anomer at 4.71 p.p.m. (C-1′, 102.0 p.p.m.). The α1″-linked GlcNAc ring of TUN has been previously assigned from a time-resolved 1-D TOCSY experiment, and in particular the 6′′-CH_2OH methylene protons are readily observed in DEPT and HSQC spectra (H-6′′a, 3.93 p.p.m.; H-6′′b, 3.82 p.p.m.; C-6′′, 63.2 p.p.m.).[11] These GlcNAc 6-hydroxymethylene signals are entirely absent for the NMR data of QVM, but the corresponding QuiNAc 6-methyl group is apparent as a proton doublet at 1.25 p.p.m. (H-6′′, 1.25 p.p.m.; $J_{5'',6''}$, 6.2 Hz; C-6′′, 17.0 p.p.m.). The TOCSY data correlates this 6-methyl group with protons signals at 4.03, 3.05, 3.62, 3.87 and 4.88 p.p.m. (Figure 5a), and NMR-HSQC C-H correlations define the QuiNAc C-1′′–C-6′′ carbon signals (Figure 5b). Notably, the anomeric signals for the QuiNAc ring are characteristic of an α-linked glycoside (H-1′′, 4.88 p.p.m.; $J_{1'',2''}$, 3.5 Hz, d; C-1′′, 99.4 p.p.m.) and the H-2′′/C-2′′ signals are characteristic for a 2-deoxy-2-*N*-acetylated sugar (H-2′′, 3.87 p.p.m.; $J_{2'',3''}$, 7.9 Hz; $J_{2'',1''}$, 3.6 Hz, dd; C-2′′, 53.7 p.p.m.). We also note that these assignments correspond closely with those recently published for the D-QuiNAc sugar of UDP-D-QuiNAc (Supplementary information, Table S1).[26,27] Hence, the NMR data confirm that the QVMs contain an α1′′, β11′-*N*-acetylquinovosamine ring in place of the GlcNAc residue for TUNs. Other NMR assignments are essentially identical for the QVMs and TUNs, with the uracil motif confirmed by the characteristic H5 and H-6 signals, the 11-carbon tunicamine dialdose by the two anomeric signals H-1′/C-1′ and H11′/C11′, and the 2,3-unsaturation in the *N*-acyl chain from the H-2′′′/C-2′′′ and H3′′′/C3′′′ signals (Supplementary information, Table S1).

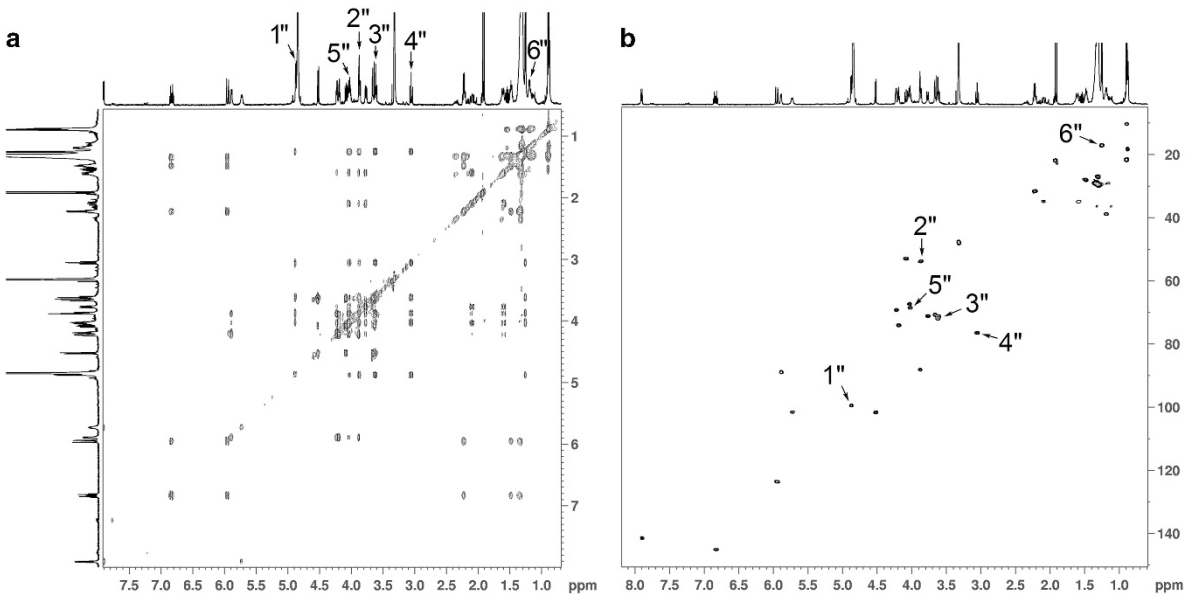

Figure 5 Homonuclear (TOCSY) (**a**) and heteronuclear (HSQC). (**b**) NMR correlation spectra of HPLC-purified quinovosamycins. The assignments for the α1″-linked *N*-acetylquinovosamine (QuiNAc) ring are as numbered. The complete assignments and comparisons with UDP-QuiNAc are shown in Supplementary information, Table S1. A full color version of this figure is available at *The Journal of Antibiotics* journal online.

Antimicrobial activity and inhibition of protein *N*-glycosylation by QVM and TUN

Naturally occurring TUNs inhibit the polyprenyl phosphate *N*-acylhexosamine 1-phosphate transferase (PPHP) superfamily, which includes bacterial translocases involved in synthesis of cell walls and capsular polysaccharides and the GlcNAc phosphotransferase (GPT) involved in eukaryotic protein *N*-glycosylation.[28–32] Hence, TUNs are generally considered toxic to all three domains of life, but with quite different mechanisms of action.[33] The specificity for this inhibition is at least partly determined by the 1″,11′-linked D-GlcNAc head group of the natural TUNs, which mimics the UDP-D-HexNAc sugar nucleotide substrates for the various members of the PPHP family.[34,35] Because the QVMs contain a different 1″,11′-linked HexNAc head group to the TUNs we sought to assess their relative antimicrobial activity (Figure 6). We used two assays to assess this, an agar diffusion assay and a broth dilution assay, using *Bacillus subtilis*, *Pseudomonas aeruginosa* and *Saccharomyces cerevisiae* as target species. The gram-positive organism *B. subtilus* is often used as a reporter strain for TUN activity, and this susceptibility is known to be conferred by the TagO-catalyzed step in teichioate cell wall biosynthesis.[36–38] *P. aeruginosa* is considered to be less susceptible, but certain strains produce capsular polysaccharides terminating in either D-FucNAc or D-QuiNAc,[39,40] either of which might be more specifically susceptible to the QVMs. The saccharomycete yeast is used as a model eukaryote, which is also reported to be susceptible to TUNs.[28] On each of these organisms we observed almost equal activity for the TUNs and QVMs. Quantitatively, *B. subtilis* and *S. cerevisiae* were readily inhibited at 0.5 μg ml^{-1} by either compound in the agar diffusion assay, whereas *P. aeruginosa* was not susceptible, even at 10-fold higher concentrations (Figures 6a–c). In the broth dilution assays, the MICs of TUN for *B. subtilis* and *S. cerevisiae* were 16 and 0.25 μg ml^{-1}, respectively, and for QVM were 128 and 0.25 μg ml^{-1}, respectively.

To investigate the mechanism of action for the antimicrobial activity we tested QVM and TUN for the ability to inhibit protein *N*-glycosylation. A transgenic *Pichia* strain expressing a heterologous *N*-glycoprotein was treated with QVM or TUN, and the secreted protein fractions were collected and assayed by gel electrophoresis.[41] The glycosylation of the glycoprotein running at 30–50 kDa is inhibited by QVM and TUN giving rise to the non-glycosylated apoprotein at 28 kDa (Figure 6d). These also co-migrate with the control *N*-glycoprotein after enzymatic de-glycosylation (Figure 6d). Hence, we report that in the yeast *Pichia*, QVM and TUN both inhibit protein *N*-glycosylation.

DISCUSSION

Four new TUN-producing strains, of which *Streptomyces niger* NRRL B-3857 is unique in that it co-produces QVMs

Naturally occurring TUNs are a diverse family of uridyl nucleoside antibiotics that include TUNs, streptovirudins and corynetoxins, and are known to be produced by a relatively diverse group of actinomycetes. The chemical structures of ten TUNs, ten streptovirudins and 14 corynetoxins are known at present.[8] These differ predominantly in the length, stereochemistry and the degree of unsaturation or hydroxylation of the *N*-linked acyl group, although streptovirudins have also been isolated in which the uracil group is replaced by dihydrouracil, without significant loss of activity. All of these compounds have in common the 11-carbon tunicamine core sugar, and the α,β-1″, 11′-linked GlcNAc residue. In the present work, we found that *S. niger* NRRL B-3857 and *Streptomyces* spp. NRRL F-4474 also produce typical TUNs Tun-15:1, Tun-16:1 and Tun-17:1 with fatty acid chains containing a conjugated double bond. However, *S. niger* NRRL B-3857 also produces novel QVMs in which the TUN GlcNAc head group is replaced by QuiNAc. To the best of our knowledge this is the first example of TUN family members in which the sugar residue is different.

The α,β-1,11-QuiNAc head group on the QVM is relevant to the biosynthetic pathway for the TUNs.

The biosynthesis of TUNs has been studied in some detail,[12,20] and is remarkable in involving the sugar nucleotide UDP-GlcNAc in two

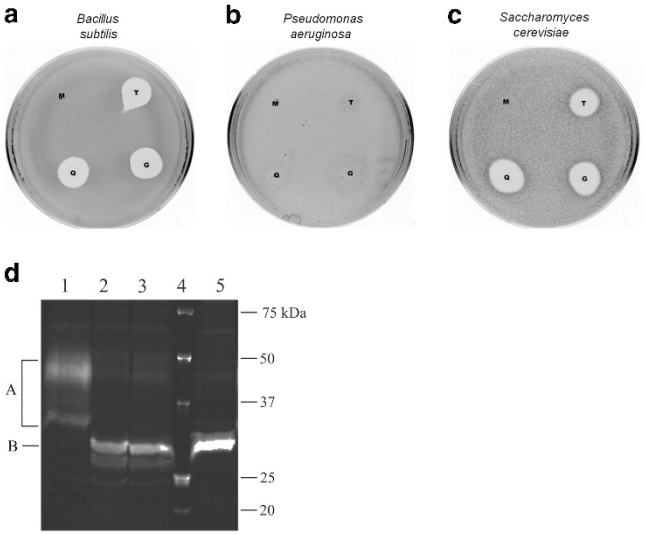

Figure 6 Agar diffusion assays and protein *N*-glycosylation assay for QVM and TUN. The inhibitors (T, commercial TUN; Q, QVM from B-3857; and G, TUN from B-3857) are tested at at 0.5 μg ml^{-1} against *B. subtilis* MW10 (**a**) and *S. cerevisiae* NRRL Y-2034 (**c**), and at 5 μg ml^{-1} against *P. aeruginosa* ATCC 27853 (**b**). The control, M, is methanol. Broth dilution assays are presented as Supplementary information. (**d**) SDS-PAGE analysis of heterologous AtchitIV5 *N*-glycoprotein expressed by *Pichia*. Lane 1. control; 2.+TUN, 20 μg ml^{-1}; 3.+QVM, 20 μg ml^{-1}; 4. mass standards; 5. AtchitIV5 after *in vitro* de-glycosylation with PNGase. A. Glycoprotein, B. non-glycosylated apoprotein. A full color version of this figure is available at *The Journal of Antibiotics* journal online.

different roles (Figure 7). First, under the influence of the putative dehydratase TunA, UDP-GlcNAc is converted to an exo-glycal intermediate, UDP-GlcNAc-5,6-ene. This is epimerized via TunF to a galactopyranosyl configuration, UDP-GalNAc-5,6-ene, which is a direct precursor of the first 11-carbon sugar nucleotide, UDP-tunicaminyl-uracil (Figure 7). Noticeably, a hypothetical 5,6-reductase can be postulated to reduce the UDP-GlcNAc-5,6-ene directly to UDP-D-QuiNAc as a possible precursor for the QVMs. In the known TUN pathway the second exo-glycal intermediate, UDP-GalNAc-5,6-ene, reacts with a uridine 5′-radical in a step catalyzed by TunB to form the 11-carbon backbone of UDP-tunicamine-uracil. However, the UDP-GalNAc-5,6-ene is considered to be less likely to be a substrate for the postulated 5,6-reductase step, which would give rise to UDP-D-FucNAc, because we were unable to detect QVMs from *S. niger* with a D-FucNAc head group. The second involvement of UDP-GlcNAc in the TUN pathway is as a glycosyl donor, as a precursor for the formation of the α,β-1″,11′-GlcNAc group. This formation of an α,β-1,1-anomer-to-anomeric glycosidic linkage is highly unusual, and is most probably catalyzed by the putative glycosyltransferase TunD, using UDP-D-GlcNAc as the glycosyl donor. Clearly, if the UDP-D-QuiNAc generated earlier in the pathway were to substitute as the substrate for TunD this could lead to both TUNs and QVM, as indeed we find for the fermentation products of *S. niger* NRRL B-3857. Whether it is the availability of UDP-QuiNAc in *S. niger* that determines QVM production, or a relaxed substrate specificity of TunD is as yet unknown, as is the specificity of other TunD proteins for UDP-QuiNAc versus UDP-GlcNAc. A more detailed understanding of possible TunD homologs in *S. niger* will undoubtedly aide in elucidating this biosynthesis, and this study is currently underway.

Compared with the TUNs, the QVMs have unexpected antimicrobial activity on *Saccharomyces* yeast and on *Bacillus subtilis*

Several questions remain unanswered concerning the inhibitory specificity of the QVMs. In eukaryotes, the TUNs inhibit the enzyme GPT, which catalyzes the transfer of *N*-acetylglucosamine-1-phosphate from UDP-N-acetylglucosamine (UDP-GlcNAc) to a membrane-bound polyprenol carrier, dolichol phosphate. The enzyme is highly selective for UDP-GlcNAc, and indeed TUN act as a tight binding competitive inhibitor because it resembles this donor nucleotide sugar. We are therefore surprised to find that the QVMs have almost equal antimicrobial activity against *S. cerevisiae* as do the TUNs. This might suggest that the yeast GPT enzyme is less selective for the TUN 1″, 11′-GlcNAc-motif than expected, and might also accommodate the QVM 1″,11′-QuiNAc residue. In support of this, we also showed that QVM and TUN have similar inhibitory activity in a yeast protein *N*-glycosylation assay, indicating that they have the same mechanism of action. This has consequences on the general substrate specificity of eukaryotic GPT because, to the best of our knowledge, dolichol-PP-QuiNAc intermediates have not been reported in eukaryotes, and the Asn-linked sugar residue for eukaryotic protein *N*-glycosylation is generally considered to be highly selective for GlcNAc.[42,43]

Besides eukaryotic GPT, TUN also inhibits bacterial translocases in the PNPT superfamily. These include the MraY, WecA, TagO, WbcO, WbpL and RgpG families that are responsible for early steps in the synthesis of bacterial cell wall components such as the *O*-antigen and teichoic acid, and of several capsular polysaccharides. These bacterial translocases typically use undecaprenol phosphate as the acceptor substrate, but differ in their specificity for the UDP-sugar donor substrate. The structural basis for this sugar nucleotide specificity is uncertain, but potential carbohydrate recognition domains have been identified within the C-terminal cytoplasmic loops of MraY, WecA and WbpL that are highly conserved in family members with the same UDP-*N*-acetylhexosamine specificity.[34,35] The related integral membrane proteins WecA and TagO are directly analogous in their sugar nucleotide usage to the eukaryotic GPT enzyme, and transfer GlcNAc-1-P to form undecaprenol-PP-GlcNAc. MraY catalyzes the transfer of the peptidoglycan precursor phospho-MurNAc-pentapeptide from UDP-D-MurNAc-pentapeptide to the polyprenol carrier undecaprenyl phosphate, an essential step of bacterial cell wall biosynthesis. TUN is a reversible, competitive inhibitor of MraY with respect to the sugar nucleotide substrate, but is non-competitive with the polyprenol phosphate motif,[44] indicating that TUN competes with the UDP-HexNAc for binding at the active site. This has led to the suggestion that TUNs with different 1″,11′-linked D-HexNAc headgroups may have altered specificity toward various members of this enzyme family. Interestingly, we found that TUNs and QVMs have essentially the same antibacterial activity against *B. subtilis*, indicating that QuiNAc may effectively substitute for GlcNAc on the TUN backbone and yet retain the inhibitory effect against this bacterium.

Some serotypes of *P. aeruginosa* have QuiNAc in their *O*-antigen and may possess a WbpL-like transferase that uses UDP-QuiNAc as the sugar nucleotide substrate.[40,45] The gene *wbpL* has been found in the *O*-antigen biosynthetic gene cluster in several *P. aeruginosa* serogroups.[40,46] WbpL initiates the biosynthesis of both the common and the serotype-specific LPS antigen by transferring GlcNAc-1-P or FucNAc-1-P to undecaprenol-P.[39,47] The structural feature of the D-QuiNAc head group might suggest that QVM will be a more potent inhibitor of the WbpL-type translocases than TUN. However, we

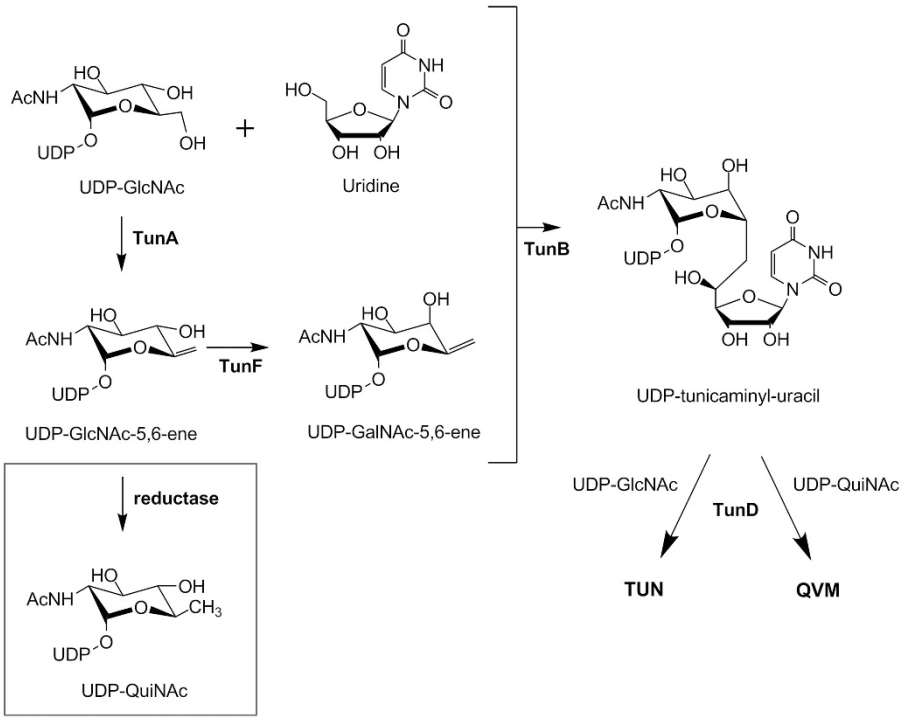

Figure 7 Biosynthesis of QVM and TUN. Exo-glycal intermediates UDP-GlcNAc-5,6-ene and UDP-GalNAc-5,6-ene are incorporated into the 11-carbon sugar nucleotide intermediate, UDP-tunicamine-uracil, which is the acceptor substrate for the putative TunD α1″,11′-glycosyltransferase. The donor substrate specificity of TunD may determine the production of QVM and TUN. The UDP-GlcNAc-5,6-ene is also a potential precursor for the UDP-QuiNAc. A full color version of this figure is available at *The Journal of Antibiotics* journal online.

noted that neither QVM nor TUN had significant antibacterial activity against *P. aeruginosa*, and whether there is selective blocking of the *Pseudomonas O*-antigen terminating in D-QuiNAc by the QVMs will therefore require further investigation.

MATERIALS AND METHODS

Materials, bacterial strains and culturing conditions

Streptomyces spp. NRRL F-4474, *S. niger* NRRL B-3857 (formally *Chainia nigra*), *S. chartreusis* NRRL 3882, *S. chartreusis* NRRL 12338 and *S. cerevisiae* strain NRRL Y-2034 were obtained from the ARS Microbial Collection housed in Peoria, IL, USA. *B. subtilis* strain MW10 was obtained from the Bacillus Genetic Stock Center (Ohio State University, Columbus, OH, USA). The actinomycetes strains were maintained on solid TYD agar (1.5%), and grown aerobically in liquid TYD medium (tryptone (2 g l^{-1}), yeast extract (2 g l^{-1}), glucose (6 g l^{-1}) and $MgCl_2.6H_2O$ (0.3 g l^{-1}) at 28 °C as described previously.[12] After 8–10 days of growth, the acid-insoluble QVM (or TUN) complex was precipitated by acidifying the cultures (0.2 M HCl). Cell pellets and the acid precipitate were collected by centrifugation (4000 *g*, 10 min) and extracted by vortexing with methanol. Following centrifugation to remove cell debris, the methanolic supernatant was evaporated to dryness (40 °C). Further purification was achieved by reversed-phase HPLC as described below. All chemicals, reagents and solvents used were obtained from Sigma-Aldrich, St Louis, MO, USA.

Reversed-phase HPLC purification

Acid-precipitated material from whole-cell cultures was methanol extracted and purified by C18 reversed-phase HPLC, essentially as described previously.[22] The instrument used was a Finnigan Surveyor system (ThermoFisher Scientific, West Palm Beach, FL, USA). The chromatography was achieved on a Spheri-5 ODS column (250 mm, 5-mm particle size) eluted with a solvent gradient from 45–55% aqueous acetonitrile for 15 min at a flow rate of 1 ml min^{-1}. The detection was by diode array, and samples were collected manually from multiple injection runs.

Bioinformatics techniques

Draft genome sequences of *Streptomyces* strains determined by Doroghazi *et al.*[3] and others, were obtained from GenBank and uploaded into the sequence bin for the respective strain entries in the isolate database of the Bacterial Isolate Genome Sequence Database system (BIGSdb) version 1.10.1[48] hosted on the ARS Microbial Genome Sequence Server (http://199.133.98.43). The gene sequences for the genes involved in the TUN biosynthetic pathway in *Streptomyces chartreusis* NRRL B-3882[14] were downloaded from GenBank (HQ111437) and were used to define loci to be searched in the Sequences/Sequence Definition database of BIGSdb. The genome sequences of all 336 isolate records having draft genome sequences were then scanned for the presence of alleles of the *tunA* through *tunL* genes using the gene sequences from NRRL B-3882 to perform BLAST searches against the draft genomes. The new or existing alleles of various house-keeping genes and the TUN biosynthetic genes were tagged within the genome sequence by the database software.

Carbohydrate derivatization for GC/MS analysis

HPLC-purified samples (about 5 mg) were acid hydrolyzed to component aldose monosaccharides (2 M trifluoroacetic acid, 121 °C, 1 h). After derivatization with hydroxylamine hydrochloride in pyridine, the samples are PAANs and analyzed by GC/MS.[49] The GC/MS analyses used a Shimadzu GC 2010 Plus gas chromatograph equipped with an AOC 20i autoinjector (Shimadzu Scientific Instruments, Addison, IL, USA). The GC is interfaced with a Shimadzu QP2010 Ultra mass-selective detector configured in EI mode. Chromatography was accomplished with a capillary HP-1 column (30 m; 0.25 mm). Helium (18.6 ml min^{-1}) is the carrier gas. The oven temperature was ramped over a linear gradient from 150 to 250 °C at 4 °C min^{-1}. Injector

and detector/interface temperatures were 275 and 300 °C, respectively. EI Mass spectra were recorded in positive ion mode.

Permethylation analysis of the fermentation products

An aliquot of the HPLC-purified fermentation extracts was removed. Permethylation was performed according to the method of Ciucanu and Kerek,[50] with modifications to limit oxidative degradation.[51] Where indicated, peracetylation of the fermentation products was achieved with acetic anhydride: pyridine (1:1 v/v, 60 °C, 20 min) as described previously.[49]

Analysis by C18-HPLC-MS^n

MS samples (2 µl injection) were analyzed by LC-MS (Thermo Accela HPLC, Thermo Fisher Scientific, Waltham, MA, USA) through a narrow-bore (2.1 mm × 150 mm, 3 µm particle size) C18 column (Inertsil, GL Sciences, Torrance, CA, USA) running a gradient elution of 60% A:40% B (buffer A 0.1% formic acid, buffer B 100% acetonitrile) to 0% A:100% B over 40 min at a flow rate of 250 µl min^{-1}, followed by a 1-min B washout and 10-min re-equilibration, while maintaining a constant column temperature of 30 °C. Electrospray positive mode ionization data were collected with a linear ion-trap-Orbitrap mass spectrometer (Thermo LTQ-Orbitrap Discovery, Waltham, MA, USA) under Xcalibur 2.1 control. Prior to LC-MS^n experiments the instrument was tuned and calibrated using the LTQ tune mix. The fragmentation energy (CID) was set to a normalized value of 35, as this provided informative fragmentation from both native TUN standard and permethylated TUN. MS data were collected in both linear ion-trap mode and FT-Orbitrap mode, extracted ion chromatograms from Orbitrap data using a 1 *m/z* window for each composition are reported. Only linear ion-trap data was used for LC-MS^n analysis due to the faster analysis speeds. The instrument was assigned a parent ion list for MS^2 selection (for native samples: *m/z* 815.2 (Q1); 817.2 (T0); 829.3 (Q2); 831.2 (T1); 843.2 (Q3); 845.3 (T2); 857.2 (Q4); 859.3 (T3) and for permethylated samples: *m/z* 963.6 (Q1); 977.6 (Q2); 991.6 (Q3); 993. 6 (T1); 1007.6 (T2); 1021.6 (T3). MS^3, MS^4, and MS^5 ion selections for fragmentation were based on the highest intensity ion from the previous fragmentation cycle. All structures were confirmed by *de novo* interpretation of the tandem and MS^n fragmentation data.

Matrix-assisted laser desorption/ionization-time-of-flight MS

MALDI-TOF MS were recorded on a Bruker-Daltonic Microflex (Billerica, MA, USA) instrument operating in reflectron mode. Ion source 1 was set to 19.0 kV, and source 2 to 14.0 kV, with lens and reflector voltages of 9.20 and 20.00 kV, respectively. Laser excitation was set to 337.1 nm, typically at 60% of 150 µJ maximum output, and 3000 shots were accumulated. The matrix use was 2,5-dihydrobenzoic acid.

Nuclear magnetic resonance

NMR spectra were obtained on a Bruker Avance spectrometer (Bruker BioSpin, Billerica, MA) operating at 500.11 Mhz using a 5 mm z-gradient BBI probe at 27 °C. Chemical shifts are reported as ppm from TMS calculated from the lock solvent.

Agar diffusion assay

Antibacterial activity of TUN and QVM was measured qualitatively by agar diffusion. *B. subtilis* strain MW10 was obtained from the Bacillus Genetic Stock Center (Ohio State University, Columbus, OH), and *S. cerevisiae* strain NRRL Y-2034 was obtained from the ARS Culture Collection maintained at the USDA-ARS National Center for Agricultural Utilization Research, Peoria, IL. *P. aeruginosa* ATCC 27853 was from the American Type Culture Collection (Manassas, VA, USA). Bacterial cultures were grown on TSB (tryptic soy broth) medium, and cultures of *S. cerevisiae* were grown on YPD (yeast extract peptone dextrose) medium. Bacteria or yeast were adjusted to a density of 0.5 McFarland's unit, diluted 1:100 in 10 ml of molten (45 °C) 1% agar media (either TSB or YPD) and poured on an agar plate (100 × 15 mm) of its respective media. After the agar had cooled and congealed, an aliquot (5 µl of either 0.1 or 1.0 ml min^{-1} TUN or QVM) was applied to the surface. Plates were incubated aerobically at 37 °C overnight, and scored for a zone of growth inhibition at the site of application.

Broth dilution assay for measuring the MIC values

MICs were determined by a modification of the broth microdilution method (National Committee for Clinical Laboratory Standards, 2002). Serial twofold dilutions of TUN or QVM in growth media were made in the wells of a 96-well plate. Each well was inoculated with the target organism (~10^5 CFU ml^{-1}), and plates incubated at 37 °C. Plates were scored for the lowest concentration of TUNs or quinovosamycins that completely inhibited growth of the target strain.

Protein glycosylation bioassays

A strain of the methylotrophic yeast *Pichia pastoris*, engineered to secrete a recombinant plant chitinase (UniProt: Q9M2U5.1; NCBI Accession: AAQ62423.1), was used in the assay.[41] Cultures were grown and proteins expressed as described previously for a human lipase-related glycoprotein[52] except that chitinase was expressed at 25 °C for 8 h. QVM or TUN was added to expression media at 20 µg ml^{-1}. After expression, proteins were concentrated from cell-free media with Amicon ultra centrifugal filters (EMD-Millipore). An aliquot of concentrated proteins from the control culture was treated with PNGaseF (New England Biolabs, Ipswich, MA, USA) to remove carbohydrates prior to gel loading. Concentrated proteins were separated by SDS-PAGE, stained with oriole fluorescent stain (Bio-Rad, Hercules, CA, USA) and visualized with a Gel-Doc EZ imager (Bio-Rad).

CONFLICT OF INTEREST

The authors declare no conflict of interest.

ACKNOWLEDGEMENTS

We thank Trina Hartman for technical assistance, Euan Price for help with drafting figures, and Dr Joseph Rich (USDA, NCAUR, Peoria, IL, USA) for pre-review of the manuscript. Mention of trade names or commercial products in this publication is solely for the purpose of providing specific information and does not imply recommendation or endorsement by the U.S. Department of Agriculture. USDA is an equal opportunity provider and employer.

Author contributions: DPL, TAN and WWM designed, administered and performed the genomic database and searches. TAN also undertook the protein *N*-glycosylation assays. KEV provided analysis by NMR. MJB and MAB undertook permethylation and MS analysis. KMB designed and performed the antimicrobial assays. NPJP conceived the experiments, analyzed data and wrote the paper.

1 Walsh, C. T. & Wencewicz, T. A. Prospects for new antibiotics: a molecule-centered perspective. *J. Antibiot.* **67**, 7–22 (2014).
2 Challis, G. L. Mining microbial genomes for new natural products and biosynthetic pathways. *Microbiology* **154**, 1555–1569 (2008).
3 Doroghazi, J. R. *et al.* A roadmap for natural product discovery based on large-scale genomics and metabolomics. *Nat. Chem. Biol.* **10**, 963–968 (2014).
4 Ju, K.-S., Doroghazi, J. R. & Metcalf, W. W. Genomics-enabled discovery of phosphonate natural products and their biosynthetic pathways. *J. Ind. Microbiol. Biotechnol.* **41**, 345–356 (2014).
5 Wang, H., Fewer, D. P., Holm, L., Rouhiainen, L. & Sivonen, K. Atlas of nonribosomal peptide and polyketide biosynthetic pathways reveals common occurrence of non-modular enzymes. *Proc. Natl Acad. Sci. USA* **111**, 9259–9264 (2014).
6 Zhang, Q., Doroghazi, J. R., Zhao, X., Walker, M. C. & van der Donk, W. A. Expanded natural product diversity revealed by analysis of lanthipeptide-like gene clusters in *Actinobacteria*. *Appl. Environ. Microbiol.* **81**, 4339–4350 (2015).
7 Tamura, G. *Tunicamycin*, Japan Scientific Societies Press, Tokyo, Japan, (1982).
8 Eckardt, K. Tunicamycins, streptovirudins, and corynetoxins, a special subclass of nucleoside antibiotics. *J. Nat. Prod.* **46**, 544–550 (1983).
9 Price, N. P. J. & Tsvetanova, B. C. Biosynthesis of the tunicamycins: a review. *J. Antibiot.* **60**, 485–491 (2007).
10 Brandish, P. E. *et al.* Modes of action of tunicamycin, liposidomycin B, and mureidomycin A: inhibition of phospho-*N*-acetylmuramyl-pentapeptide translocase from *Escherichia coli*. *Antimicrob. Agents Chemother.* **40**, 1640–1644 (1996).
11 Xu, L., Appell, M., Kennedy, S., Momany, F. A. & Price, N. P. Conformational analysis of chirally deuterated tunicamycin as an active site probe of UDP-*N*-acetylhexosamine:

polyprenol-P *N*-acetylhexosamine-1-P translocases. *Biochemistry* **43**, 13248–13255 (2004).
12 Tsvetanova, B. C., Keimle, D. J. & Price, N. P. J. Biosynthesis of tunicamycin and metabolic origin of the 11-carbon dialdose sugar, tunicamine. *J. Biol. Chem.* **277**, 35289–35296 (2002).
13 Wyszynski, F. J., Hesketh, A. R., Bibb, M. J. & Davis, B. G. Dissecting tunicamycin biosynthesis by genome mining: cloning and heterologous expression of a minimal gene cluster. *Chem. Sci.* **1**, 581–589 (2010).
14 Chen, W. *et al.* Characterization of the tunicamycin gene cluster unveiling unique steps involved in its biosynthesis. *Protein Cell* **1**, 1093–1105 (2010).
15 Boyle, D. S. & Donachie, W. D. *mraY* is an essential gene for cell growth in *Escherichia coli*. *J. Bacteriol.* **180**, 6429–6432 (1998).
16 Kimura, K.-I. & Bugg, T. D. H. Recent advances in antimicrobial nucleoside antibiotics targeting cell wall biosynthesis. *Nat. Prod. Rep.* **20**, 252–273 (2003).
17 Dini, C. MraY inhibitors as novel antibacterial agents. *Curr. Top. Med. Chem.* **5**, 1221–1236 (2005).
18 Doroghazi, J. R. *et al.* Genome sequences of three tunicamycin-producing streptomyces strains, *S. chartreusis* NRRL 12338, *S. chartreusis* NRRL 3882, and *S. lysosuperificus* ATCC 31396. *J. Bacteriol.* **193**, 7021–7022 (2011).
19 Kapley, A. *et al.* Antimicrobial activity of *Alcaligenes* sp. HPC 1271 against multidrug resistant bacteria. *Funct. Integr. Genomics* **16**, 57–65 (2015).
20 Wyszynski, F. J. *et al.* Biosynthesis of the tunicamycin antibiotics proceeds via unique exo-glycal intermediates. *Nat. Chem.* **4**, 539–546 (2012).
21 Luo, Q., Hiessl, S., Poehlein, A. & Steinbüchel, A. Microbial gutta-percha degradation shares common steps with rubber degradation by *Nocardia nova* SH22a. *Appl. Environ. Microbiol.* **79**, 1140–1149 (2013).
22 Tsvetanova, B. C. & Price, N. P. J. Liquid chromatography-electrospray mass spectrometry of tunicamycin-type antibiotics. *Anal. Biochem.* **289**, 147–156 (2001).
23 Ponpipom, M. M. & Hanessian, S. A method for the selective bromination of primary alcohol groups. *Carbohydr. Res.* **18**, 342–344 (1971).
24 Hanessian, S., Ponpipom, M. M. & Lavallee, P. Procedures for the direct replacement of primary hydroxyl groups in carbohydrates by halogen. *Carbohydr. Res.* **24**, 45–56 (1972).
25 Eckardt, K., Ihn, W., Tresselt, D. & Krebs, D. The chemical structures of streptovirudins. *J. Antibiot.* **34**, 1631–1632 (1981).
26 Li, T., Simonds, L., Kovrigin, E. L. & Noel., K. D. *In vitro* biosynthesis and chemical identification of UDP-*N*-acetyl-D-quinovosamine (UDP-D-QuiNAc). *J. Biol. Chem.* **289**, 18110–18120 (2014).
27 Hwang, S., Aronov, A. & Bar-Peled, M. The biosynthesis of UDP-D-QuiAc in *Bacillus cereus* ATCC 14579. *PLoS ONE* **10**, e133790 (2015).
28 Heifetz, A., Keenan, R. W. & Elbein, A. D. Mechanism of action of tunicamycin on the UDP-GlcNAc: dolichyl phosphate GlcNAc-1-phosphate transferase. *Biochemistry* **18**, 2186–2192 (1979).
29 Price, N. P. & Momany, F. A. Modeling bacterial UDP-HexNAc: polyprenol-P HexNAc-1-P transferases. *Glycobiology* **15**, 29–42 (2005).
30 Imperiali, B., O'Connor, S. E., Hendrickson, T. & Kellenberger, C. Chemistry and biology of asparagines-linked glycosylation. *Pure Appl. Chem.* **71**, 777–787 (1999).
31 Lehrman, M. A. Biosynthesis of *N*-acetylglucosamine-P-P-dolichol, the committed step of asparagine-linked oligosaccharide assembly. *Glycobiology* **1**, 553–623 (1991).
32 Lehrman, M. A. A family of UDP-GlcNAc/MurNAc: polyisoprenol-P GlcNAc/MurNAc-1-P transferases. *Glycobiology* **4**, 768–771 (1994).
33 Bugg, T. D. H. & Brandish, P. E. From peptidoglycan to glycoproteins: common features of lipid-linked oligosaccharide biosynthesis. *FEMS Microbiol. Lett.* **119**, 255–262 (1994).
34 Anderson, M. S., Eveland, S. & Price, N. P. J. Conserved cytoplasmic motifs that distinguish sub-groups of the polyprenol phosphate:*N*-acetylhexosamine-1-phosphate transferase family. *FEMS Microbiol. Lett.* **191**, 169–175 (2000).
35 Amer, A. O. & Valvano, M. A. Conserved amino acid residues found in a predicted cytosolic domain of the lipopolysaccharide biosynthetic protein WecA are implicated in the recognition of UDP-*N*-acetylglucosamine. *Microbiology* **147**, 3015–3025 (2001).
36 Swoboda, J. G., Campbell, J., Meredith, T. C. & Walker, S. Wall teichoic acid function, biosynthesis, and inhibition. *ChemBioChem* **11**, 35–45 (2010).
37 Soldo, B., Lazarevic, V. & Karamata, D. *tagO* is involved in the synthesis of all anionic cell-wall polymers in *Bacillus subtilis* 168. *Microbiology* **148**, 2079–2087 (2002).
38 Hancock, I. C., Wiseman, G. & Baddiley, J. Biosynthesis of the unit that links teichoic acid to the bacterial wall: inhibition by tunicamycin. *FEBS Lett.* **69**, 75–80 (1976).
39 Belanger, M., Burrows, L. L. & Lam, J. S. Functional analysis of genes responsible for the synthesis of the B-band *O* antigen of *Pseudomonas aeruginosa* serotype O6 lipopolysaccharide. *Microbiology* **145**, 3505–3521 (1999).
40 Raymond, C. K. *et al.* Genetic variation at the *O*-antigen biosynthetic locus in *Pseudomonas aeruginosa*. *J. Bacteriol.* **84**, 3614–3622 (2002).
41 Naumann, T. A. & Price, N. P. J. Truncation of class IV chitinases from *Arabidopsis* by secreted fungal proteases. *Mol. Plant Pathol.* **13**, 1135–1139 (2012).
42 Schwarz, F. & Aebi, M. Mechanisms and principles of *N*-linked protein glycosylation. *Curr. Opin. Struct. Biol.* **21**, 576–582 (2011).
43 Larkin, A. & Imperiali, B. The expanding horizons of asparagine-linked glycosylation. *Biochemistry* **50**, 4411–4426 (2011).
44 Chung, B. C. *et al.* Crystal structure of MraY, an essential membrane enzyme for bacterial cell wall synthesis. *Science* **341**, 1012–1016 (2013).
45 DiGiandomenico, A. *et al.* Glycosylation of *Pseudomonas aeruginosa* 1244 pilin: glycan substrate specificity. *Mol. Microbiol.* **46**, 519–530 (2002).
46 Dean, C. R. *et al.* Characterization of the serogroup O11 O-antigen locus of *Pseudomonas aeruginosa* PA103. *J. Bacteriol.* **181**, 4275–4284 (1999).
47 Rocchetta, H. L., Burrows, L. L., Pacan, J. C. & Lam, J. S. Three rhamnosyltransferases responsible for assembly of the A-band D-rhamnan polysaccharide in *Pseudomonas aeruginosa*: a fourth transferase, WbpL, is required for the initiation of both A-band and B-band lipopolysaccharide synthesis. *Mol. Microbiol.* **28**, 1103–1119 (1998).
48 Jolley, K. A. & Maiden, M. C. J. BIGSdb: Scalable analysis of bacterial genome variation at the population level. *BMC Bioinformatics* **11**, 595 (2010).
49 Price, N. P. J. Acylic sugar derivatives for GC/MS analysis of ^{13}C-enrichment during carbohydrate metabolism. *Anal. Chem.* **76**, 6566–6574 (2004).
50 Ciucanu, I. & Kerek, F. A simple and rapid method for the permethylation of carbohydrates. *Carbohydr. Res.* **131**, 209–217 (1984).
51 Ciucanu, I. & Costello, C. E. Elimination of oxidative degradation during the per-*O*-methylation of carbohydrates. *J. Am. Chem. Soc.* **125**, 16213–16219 (2003).
52 Sebban-Kreuzer, C., Deprez-Beauclair, P., Berton, A. & Crenon, I. High-level expression of nonglycosylated human pancreatic lipase-related protein 2 in *Pichia pastoris*. *Protein Expr. Purif.* **49**, 284–291 (2006).

Supplementary Information accompanies the paper on The Journal of Antibiotics website (http://www.nature.com/ja)